CHAPTER 5

SYNCHRONY AND DESYNCHRONY IN NETWORKS OF LOCALLY COUPLED WILSON-COWAN OSCILLATORS

5.1 Introduction

In this Chapter, we study networks of locally coupled Wilson-Cowan (W-C) oscillators [Wilson and Cowan, 1972]. The W-C oscillator is a two variable system of ordinary differential equations and represents an interacting population of excitatory and inhibitory neurons. The amplitudes of the variables symbolize the proportion of each population of neurons that is active. We study these equations because they represent neuronal groups, which may be the basic processing units in the brain [Edelman, 1987]. The W-C equations have a large number of parameters, which allow for a wide range of dynamics. These equations have been used widely in modelling various brain processes [Feldman and Cowan, 1975, König and Schillen, 1991, Borisyuk et al., 1993], in creating oscillatory recall networks [Wang et al., 1990], and in exploring the binding problem [Horn et al., 1991, von der Malsburg and Buhmann, 1992, Wang, 1995]. Because of the neurophysiological importance of the W-C equations, several authors have examined their mathematical properties [Ermentrout and Cowan, 1979, Baird, 1986, Sakaguchi, 1988, Ermentrout, 1990, Cairns et al., 1993]. Of particular relevance is a study by Cairns et al. [Cairns et al., 1993], which indicates that synchronization is possible with these equations. Despite extensive studies on W-C oscillators, it remains unclear to whether or not a locally coupled network can exhibit synchrony. It is also unknown how desynchronization can be achieved in such a network.

We study locally coupled networks because globally coupled networks lack topological mappings [Sporns et al., 1989, Chawanya et al., 1993]. Specifically, in a two-dimensional network of oscillators, all-to-all couplings indiscriminately connects multiple objects. All pertinent geometrical information about each object, and about its relationships with other objects is lost. This information should be preserved if the network is to be used for segmentation and object recognition. Local couplings simply and efficiently preserve these spatial relationships.

We study W-C oscillator networks with diffusive coupling. This coupling arises naturally from the equations, but, as mentioned in Chapter 3, oscillator networks with diffusive couplings typically achieve synchrony at times proportional to n^2 (see also [Kopell and Ermentrout, 1986, Niebur et al., 1991b]). In order to achieve fast synchrony (in one cycle), we adjust parameters so that the system is near a bifurcation. This causes the interaction to create and destroy fixed points in such a manner that synchrony is quickly attained.

The two main aspects of the theory of oscillatory correlation (described in Section 1.2) are synchronization within an object, and desynchronization between objects. In our model desynchronization of multiple objects is accomplished with a global inhibitor (GI), which receives input from the entire network, and feeds back to all oscillators. The global connections serve to adjust the relative phases between oscillator groups, wherever they may be on the network. The model we present uses short range coupling to achieve synchrony, while global couplings with GI give rise to desynchronization.

The model is described in the following section. In Section 5.3, it is proven that synchrony is the globally stable solution for a line of oscillators given sufficient coupling strength, and a technique for fast entrainment is presented. GI and the dynamics of desynchronization are described in Section 5.4. Computer simulations of a two dimensional network with five objects are shown in Section 5.5. In Section 5.6 we discuss possible extensions to our model.[1]

5.2 Model Definition

The basic architecture of the model is shown in Figure 53. GI is connected to the entire network. The connections between oscillators are local. An oscillator located on a black square can only be coupled with oscillators on adjacent diagonally striped squares. The topology of the network is a rectangle, not a torus. The coupling strengths are dynamically changed on a fast time scale compared to the period of the oscillations (further discussion below). The dynamic couplings serve to increase the coupling strength between units that are active, to decrease the coupling strength between excited units and inactive units, and to decrease the connection strength between two silent units, all rapidly and temporarily.

Each functional element on the grid is a simplified W-C oscillator defined as,

$$\dot{x}_i = -x_i + H(ax_i - by_i - \phi_x + \sigma z + I_i + \rho_i(t)) + \alpha_W S_{xi} \tag{5.1.a}$$

$$\dot{y}_i = \eta\,(-y_i + H(cx_i + dy_i - \phi_y)) + \alpha_W S_{yi} \tag{5.1.b}$$

$$H(v) = (1 + exp(-v))^{-1} \tag{5.1.c}$$

The parameters have the following meanings: a and d are the values of self excitation in the x and y units respectively. b is the strength of the coupling from the inhibitory unit, y, to the excitatory unit, x. The corresponding coupling strength from x to y is given by c.

1. The majority of this work has been published in Campbell and Wang, 1996.

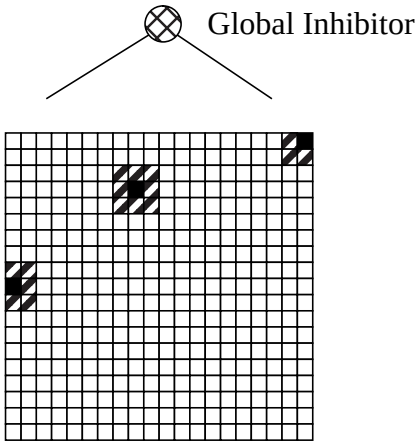

Figure 53. Basic architecture of the model. The oscillators are arranged in a 2-D grid, where each square on the grid represents an oscillator. The connections between oscillators are local. Three representative situations are shown in the figure, where an oscillator located at a black site is connected only to oscillators on adjacent striped squares. Note that we do not use periodic boundary conditions. The global inhibitor (GI) is pictured at the top and is coupled with all oscillators in the network.

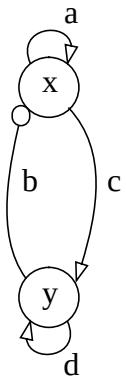

Figure 54. A diagram showing the connections that each excitatory and inhibitory unit has within an oscillator. Triangles represent excitatory connections, and circles represent inhibitory connections.

ϕ_x and ϕ_y are the biases, or thresholds. Figure 54 shows the connections for single oscillator. The x and y variables are interpreted as the average activity of the population of excitatory and inhibitory neurons respectively. η modifies the rate of change of the y unit. The coupling strength between oscillators is given by α_W. $\rho(t)$ is a noise term. The noise is assumed to be Gaussian with statistical property

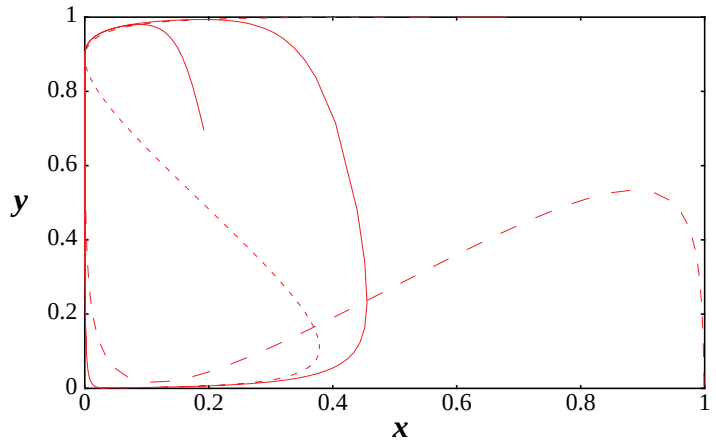

Figure 55. The y nullcline (small dashes), x nullcline (large dashes), and trajectory (solid) for a single oscillator are displayed. The parameters are $a = 10.0$, $b = 7.0$, $\phi_x = 4.075$, $c = 10.0$, $d = 10.2129$, $\phi_y = 7.0$, $\sigma = 2.1$, $\eta = 7.0$, and $D = 0$.

$$\langle \rho_i(t) \rangle = 0 \tag{5.2.a}$$

$$\langle \rho_i(t)\rho_j(t') \rangle = 2D\delta_{ij}\delta(t-t') \tag{5.2.b}$$

where D is the amplitude of the noise, $\delta(t-t')$ is the Dirac delta function, and $\delta_{ij} = 1$ if $i = j$ and 0 otherwise. The i^{th} oscillator receives a binary input I_i. A value of $I_i = 1$ corresponds to those parts of the sensory field that are stimulated and drives the oscillator into a periodic regime. Oscillators that do not receive input, namely $I_i = 0$, remain silent. z represents the activity of GI and will be specified in detail in Section 5.4. Though it may seem unusual to denote the position of an oscillator in a 2-D array with only one index, we do so to avoid using four indices to label the connections between oscillators. Figure 55 displays the nullclines, the curves along which the values of $\dot{x}$ or $\dot{y}$ are zero, and the trajectory of a point near the limit cycle. The caption of Figure 55 lists values for the parameters a, b, c, σ, η, d, ϕ_x ,ϕ_y and D.

The interaction terms are given by

$$S_{xi} = -\kappa_i x_i + \sum_j J_{ij} x_j \tag{5.3.a}$$

$$S_{yi} = -\kappa_i y_i + \sum_j J_{ij} y_j \tag{5.3.b}$$

where the sum is over $j \in N(i)$, and $N(i)$ is the set of neighbors that element i has. We call this form of coupling *scalar diffusive coupling* following the terminology of Aronson et al. [Aronson et al., 1990]. The terms $\kappa_i(t)$ and $J_{ij}(t)$ are specified below.

The connections between the oscillators are allowed to change on a fast time scale, as first suggested by von der Malsburg [von der Malsburg, 1981, von der Malsburg and Schneider, 1986]. They obey the following Hebbian rule: the connections between excited oscillators increase to a maximum, the connections between excited and unstimulated oscillators decrease to zero, and the connections between unstimulated oscillators decrease to zero. This rule uses of a pair of connection weights. The permanent links $T_{ij}'s$ denote existence of connections between i and j, and reflect the architecture of the network (locally connected 2-D grid, see Figure 53). The dynamic links J_{ij}'s change on a fast time scale compared to the period of oscillation, and represent the efficacy of the permanent links. The idea of fast synaptic modulation is introduced on the basis of its computational advantages and neurobiological plausibility [von der Malsburg, 1981, von der Malsburg and Schneider, 1986]. The permanent links are given by $T_{ij} = 1$ if i, j are neighbors and $T_{ij} = 0$ otherwise. The dynamic links are computed as follows

$$J_{ij} = T_{ij} h(\langle x_i \rangle) h(\langle x_j \rangle) \tag{5.4}$$

where $h(\langle x_i \rangle)$ is a measure of the activity of oscillator i. It is defined as $h(\langle x_i \rangle) = \Theta(\langle x_i \rangle - \varphi)$, where φ is some threshold, and Θ is the Heaviside step function. Namely $h(\langle x_i \rangle) = 1$ if the temporal average of activity, $\langle x_i \rangle$, is greater than the threshold, or $h(\langle x_i \rangle) = 0$ if otherwise. With (5.4) in place, only neighboring excited oscillators will be effectively coupled. This is an implicit encoding of the Gestalt principle of connectedness [Rock and Palmer, 1990].

With scalar diffusive coupling, the Hebbian rule defined above would destabilize the synchronous solution. To understand how the instability arises, consider three excited oscillators arranged in a row, and each with the same values of activities, i.e. $x_1 = x_2 = x_3$, and $y_1 = y_2 = y_3$. Because of the Hebbian coupling rule, the middle oscillator has the following interaction term $-\kappa_2 x_2 + x_1 + x_3 = (2 - \kappa_2) x_1$, while the first and third oscillators have the interaction terms $-\kappa_1 x_1 + x_2 = (1 - \kappa_1) x_1$ and $-\kappa_3 x_3 + x_2 = (1 - \kappa_3) x_1$ respectively. These interaction terms are different, and cause the trajectories of the oscillators to be different. An exact synchrony is not possible. An obvious solution is to change $\kappa_i(t)$ so that it equals the number of excited neighbors that oscillator i is coupled with. We set

$$\kappa_i(t) = \sum_j J_{ij}(t) \tag{5.5}$$

so that the interaction terms will be zero when the oscillators are synchronized. All the oscillators will now have the same trajectory and remain synchronous. The effect of (5.5) is similar to the *dynamic normalization* introduced by Wang [Wang, 1993a, Wang, 1995]. The original form of dynamic normalization served to normalize the connection strengths between oscillators. In this model we do not normalize connection strengths, but instead alter the multiplicative constant on the scalar diffusive coupling term. Either formulation would have the same results with these equations, but we choose to normalize the multi-

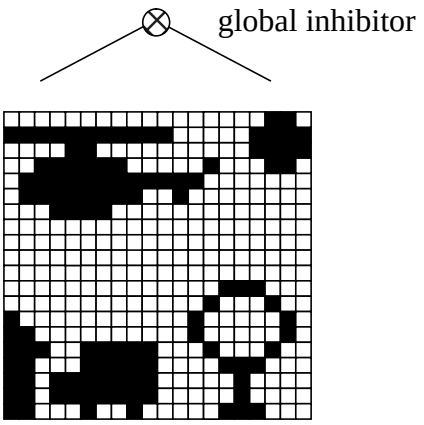

Figure 56. Input used for the network. Black squares denote oscillators that receive input. Starting clockwise from the upper left hand corner, we name the objects as follows: a helicopter, a thick addition sign, a tree, a truck, and a house.

plicative constant because it is more direct. The effect of dynamic normalization is to maintain a balanced interaction term so that coupled oscillators remain synchronous independent of the number of connections that they have.

The architecture of this network allows us to implement the basic aspects of oscillatory correlation, synchrony and desynchrony. To illustrate, assume that the network receives input as shown in Figure 56. The black squares represent units that receive stimulation, and these units then produce oscillatory behavior. The dynamic couplings will disconnect excited units from unexcited units, and group connected units together. For the five objects pictured in the input, there will be five corresponding groups of oscillators. Connected oscillators synchronize, and GI ensures that no two spatially separated objects have the same phase.

5.3 Synchronization

Much work has been done with coupled phase oscillators [Kuramoto and Nishikawa, 1987, Daido, 1988, Strogatz and Mirollo, 1988, Ermentrout, 1990, Ermentrout and Kopell, 1990, Sompolinsky et al., 1991] because the phase model is the simplest description of a smooth limit cycle. Phase oscillators are generally defined as

$$\dot{\phi}_i = \omega_i + \sum_j J_{ij} G(\phi_i, \phi_j) \tag{5.6}$$

where ϕ_i is the phase of the i^{th} oscillator, ω_i is its intrinsic frequency. J_{ij} is the coupling strength between the i^{th} and the j^{th} oscillators. For phase oscillators with local diffusive coupling, and identical intrinsic frequencies, the in-phase solution is asymptotically stable [Cohen et al., 1982]. But the phase model does not exhibit the rich variety of behaviors that other, more complex nonlinear oscillators, have when locally coupled (for example

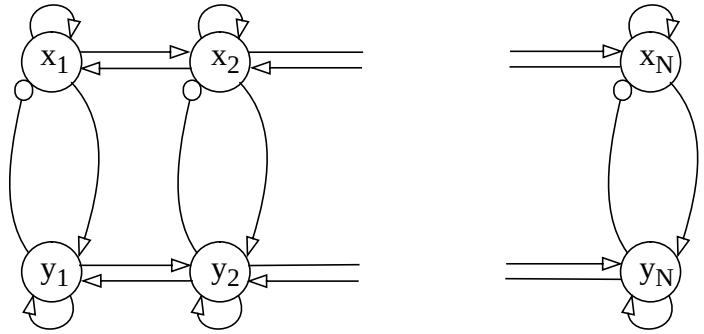

Figure 57. A diagram showing the interactions between the excitatory and inhibitory units in a chain of oscillators. See the caption of Figure 54 for the meaning of the notations.

[Schreiber and Marek, 1982, Ashkenazi and Othmer, 1978, Han et al., 1995]. Because the system of W-C oscillators that we use differs significantly from those mentioned above, we examine the properties of the following approximation to the W-C oscillator in detail. We show that with a sufficiently large coupling strength synchrony occurs for a finite number of oscillators, independent of their initial conditions.

Using basic matrix stability analysis, we show that a line of oscillators can achieve synchrony. The equations we analyze are a bit different from those shown in (5.1). We do not include parameter η, $D = 0$, and we do not consider the effects of GI. We have also dropped the S notation because the interaction terms can be explicitly included. A diagram of the connections between units, arranged in a line, is given in Figure 57. Note that the two ends are not connected with one another. Thus we are analyzing a line, not a ring, of n oscillators. The equations are

$$\dot{x}_1 = -x_1 + P(ax_1 - by_1 - \varphi_x) + \alpha_W (x_2 - x_1) \tag{5.7.a}$$

$$\dot{y}_1 = -y_1 + P(cx_1 + dy_1 - \varphi_y) + \alpha_W (y_2 - y_1) \tag{5.7.b}$$

...

$$\dot{x}_i = -x_i + P(ax_i - by_i - \varphi_x) + \alpha_W (x_{i+1} + x_{i-1} - 2x_i) \tag{5.7.c}$$

$$\dot{y}_i = -y_i + P(cx_i + dy_i - \varphi_y) + \alpha_W (y_{i+1} + y_{i-1} - 2y_i) \tag{5.7.d}$$

...

$$\dot{x}_n = -x_n + P(ax_n - by_n - \varphi_x) + \alpha_W (x_{n-1} - x_n) \tag{5.7.e}$$

$$\dot{y}_n = -y_n + P(cx_n + dy_n - \varphi_y) + \alpha_W (y_{n-1} - y_n) \tag{5.7.f}$$

where the sigmoid function $H(v)$ has been approximated with

$$P(v) = \begin{cases} 0 & if \quad v < -e \\ v/(2e) + 1/2 & if \; -e \le v \le e \\ 1 & if \quad v > e \end{cases} \tag{5.8}$$

The constants a, b, c, d, φ_x, and φ_y are positive values, $\log(e) = 1$, and α_W is the coupling strength. We now state our major analytical result as the following theorem.

Theorem *For the system of coupled oscillators defined in (5.7) and (5.8), the coupling strength α_W can be chosen such that synchrony is asymptotically stable.*

Proof: First, let $a^2 + b^2 > c^2 + d^2$, and let us define the following notations

$$\bar{r}_i = (x_i - x_{i+1}, y_i - y_{i+1}) \,,\; r_i^2 = (x_i - x_{i+1})^2 + (y_i - y_{i+1})^2 \tag{5.9}$$

$$\cos(\theta_i) = \frac{(x_i - x_{i+1})}{r_i} \text{, and } \sin(\theta_i) = \frac{(y_i - y_{i+1})}{r_i} \tag{5.10}$$

$$f_i = P(ax_i - by_i - \varphi_x) - P(ax_{i+1} - by_{i+1} - \varphi_x) \tag{5.11.a}$$

$$g_i = P(cx_i + dy_i - \varphi_y) - P(cx_{i+1} + dy_{i+1} - \varphi_y) \tag{5.11.b}$$

Note that $\bar{r}_i$ is a two element vector, and r_i is the positive square root of r_i^2. The time derivative of the distance between two oscillators can be written as

$$\frac{1}{2}\frac{d}{dt} r_i^2 = \bar{r}_i \cdot \dot{\bar{r}}_i = r_i \dot{r}_i \tag{5.12}$$

We will use the "dot" above a variable to denote its first order time derivative. According to (5.7)we can write

$$\begin{aligned} r_i \dot{r}_i = & -(1 + 2\alpha_W) r_i^2 + (r_i \cos(\theta_i) f_i + r_i \sin(\theta_i) g_i) \\ & + \alpha_W(\bar{r}_i \cdot \bar{r}_{i-1} + \bar{r}_i \cdot \bar{r}_{i+1}) \end{aligned} \tag{5.13}$$

In the above equation $1 \le i \le n-1$, and let the values of the undefined variables $r_0 = r_n = 0$. The functions f_i and g_i are bounded by

$$-1 \le f_i \le 1, \quad -1 \le g_i \le 1 \tag{5.14}$$

Thus, the second term on the RHS of is bounded by

$$-\sqrt{2} r_i \le r_i \cos(\theta_i) f_i + r_i \sin(\theta_i) g_i \le \sqrt{2} r_i \tag{5.15}$$

The last term on the RHS of is bounded by

$$-\alpha_W r_i (r_{i-1} + r_{i+1}) \le \alpha (\bar{r}_i \cdot \bar{r}_{i-1} + \bar{r}_i \cdot \bar{r}_{i+1}) \le \alpha_W r_i (r_{i-1} + r_{i+1}) \tag{5.16}$$

Using (5.15) and (5.16), an upper bound and a lower bound on can be written as

$$\begin{aligned} -(1 + 2\alpha_W) r_i^2 - \sqrt{2} r_i - \alpha_W r_i (r_{i-1} + r_{i+1}) &\le r_i \dot{r}_i \\ &\le -(1 + 2\alpha_W) r_i^2 + \sqrt{2} r_i + \alpha_W r_i (r_{i-1} + r_{i+1}) \end{aligned} \tag{5.17}$$

which now places a finite bound on r_i as a function of α and n. If $\alpha = 0$, and we divide both sides by r_i, then (5.17) becomes

$$-r_i - \sqrt{2} \le \dot{r}_i \le -r_i + \sqrt{2} \tag{5.18}$$

which implies that $\dot{r} \le 0$ if $r_i > \sqrt{2}$. Consequently, the bounds will reach an equilibrium such that r_{max}, the maximum distance between any two connected oscillators, is less than, or equal to $\sqrt{2}$. Thus, without any coupling whatsoever, there is a finite bound on r_{max}. Because the interaction terms are designed to give rise to synchrony, one would expect that they would have the effect of reducing r_{max}. We now show that we can control the size of r_{max} by an appropriate choice of α_W. We divide (5.17) by r_i and examine only the upper bound, which we rewrite as a matrix equation

$$\dot{\boldsymbol{q}} = \alpha_W \begin{bmatrix} -1/\alpha_W - 2 & 1 & & & & \\ 1 & -1/\alpha_W - 2 & 1 & & & \\ & & \cdots & & & \\ & & & 1 & -1/\alpha_W - 2 & 1 \\ & & & & 1 & -1/\alpha_W - 2 \end{bmatrix} \boldsymbol{q} + \sqrt{2}\boldsymbol{k} \tag{5.19}$$

where $\boldsymbol{q} = (q_1, q_2, \ldots, q_{n-1})^t$ and $\boldsymbol{k}$ is a $(n-1) \times 1$ column vector of all 1's. Let $\boldsymbol{A}$ be the matrix in (5.19). We will use the convention of denoting vectors with lower case bold letters, and matrices with upper case bold letters. The superscript "t" denotes the transpose. The eigenvalues of $\boldsymbol{A}$ are all negative, thus (5.19) approaches an equilibrium value at an exponential rate. The equilibrium values of the elements in $\boldsymbol{q}$, which we denote with $\boldsymbol{q}^{eq}$, are defined by

$$\boldsymbol{q}^{eq} = -\frac{\sqrt{2}}{\alpha_W} \boldsymbol{A}^{-1} \boldsymbol{k} \tag{5.20}$$

We multiply each side of (5.20) by $\boldsymbol{k}^t$ to obtain

$$\sum_{i=1}^{n-1} q_i^{eq} = -\frac{\sqrt{2}}{\alpha_W} \sum_{i,j=1}^{n-1} \left(A^{-1} \right)_{ij} \tag{5.21}$$

For $\alpha_W \gg 1$ we can approximate $\boldsymbol{A}$ with $\boldsymbol{B}$, where

$$\boldsymbol{B} = \begin{bmatrix} -2 & 1 & & & \\ 1 & -2 & 1 & & \\ & & \cdots & & \\ & & 1 & -2 & 1 \\ & & & 1 & -2 \end{bmatrix} \tag{5.22}$$

The inverse of this matrix follows a regular pattern and we can explicitly write

$$-\sum_{i,j=1}^{n-1} \left(B^{-1} \right)_{ij} = \frac{1}{2} + \frac{11}{12}(n-1) + \frac{1}{2}(n-1)^2 + \frac{1}{12}(n-1)^3 \tag{5.23}$$

Because the elements of $\boldsymbol{A}^{-1}$ change continuously and monotonically with α_W (see [Bellman, 1970]), and also because $\boldsymbol{A}$ remains invertible in the range $0 \le \alpha_W < \infty$, we can use (5.23) as an upper bound on the sum of all the elements in $\boldsymbol{A}^{-1}$, i.e.

$$-\sum_{i,j=1}^{n-1} \left(A^{-1} \right)_{ij} < -\sum_{i,j=1}^{n-1} \left(B^{-1} \right)_{ij} \tag{5.24}$$

We use (5.23) and (5.24) to bound (5.21) as

$$\sum_{i=1}^{n-1} q_i^{eq} < \frac{\sqrt{2}}{\alpha_W} \left[\frac{1}{2} + \frac{11}{12}(n-1) + \frac{1}{2}(n-1)^2 + \frac{1}{12}(n-1)^3 \right] \tag{5.25}$$

It can be shown that the elements of matrix $\boldsymbol{A}^{-1}$ are all negative. Given that the elements of $\boldsymbol{k}$ are all 1's, (5.20) implies that all the elements of $\boldsymbol{q}^{eq}$ are greater than zero. With this we can write the following inequality

$$q_{max}^{eq} \le \sum_{i=1}^{n-1} q_i^{eq} \tag{5.26}$$

where q_{max}^{eq} is the maximum of the q_i^{eq}'s. (5.26) and (5.25) give the following inequality

$$q_{max}^{eq} < \frac{\sqrt{2}}{\alpha_W} \left[\frac{1}{2} + \frac{11}{12}(n-1) + \frac{1}{2}(n-1)^2 + \frac{1}{12}(n-1)^3 \right] \tag{5.27}$$

Assume that both systems of $\boldsymbol{r}$ and $\boldsymbol{q}$ start with the same initial conditions, i.e. $\boldsymbol{r}(0) = \boldsymbol{q}(0)$. Given that $\dot{\boldsymbol{r}} \le \boldsymbol{A}\boldsymbol{r} + \sqrt{2}\boldsymbol{k}$ and $\dot{\boldsymbol{q}} = \boldsymbol{A}\boldsymbol{q} + \sqrt{2}\boldsymbol{k}$, it is known that $\boldsymbol{r}(t) \le \boldsymbol{q}(t)$ for $t \ge 0$ [Golomb and Shanks, 1965]. Thus, after some time, (5.18) will reach equilibrium, and we can use (5.27) and that $r_{max} \le q_{max}$ to write

$$r_{max} < \frac{\sqrt{2}}{\alpha_W}\left[\frac{1}{2} + \frac{11}{12}(n-1) + \frac{1}{2}(n-1)^2 + \frac{1}{12}(n-1)^3\right] \tag{5.28}$$

(5.28) shows that for fixed n, r_{max} is bounded by a quantity that is inversely proportional to α_W. In essence, we can decrease r_{max} by increasing α_W. We use this control to further constrain the upper bound of (5.15), because once r_{max} is smaller than a certain value,

$$r_f = \frac{2e}{\left(a^2 + b^2\right)^{1/2}} \tag{5.29}$$

the maximal values for f_i and g_i are no longer equal to 1. According to (5.8) and (5.11), if $f_i = 1$ then one oscillator is at a location on the plane such that $ax_1 - by_1 - \varphi_x > e$, and the other oscillator must satisfy $ax_2 - by_2 - \varphi_x < -e$. In other words, the oscillators lie on opposite sides of the piece-wise linear function $P(v)$, and do not lie on the intermediate sloped line. r_f is the minimum distance between two oscillators such that $f_i = 1$. If the distance between two oscillators is less than r_f, then the two oscillators lie on the same, or adjacent, pieces of function $P(v)$ and thus $f_i < 1$. There is also a corresponding value r_g for the function g_i, but $r_f < r_g$ due to the constraint $a^2 + b^2 > c^2 + d^2$ previously mentioned. If $r_{max} < r_f$ then automatically $r_{max} < r_g$ which implies that $g_i < 1$. Thus we want to choose α_W such that

$$\alpha_W > \frac{\left(a^2 + b^2\right)^{1/2}}{\sqrt{2}e}\left[\frac{1}{2} + \frac{11}{12}(n-1) + \frac{1}{2}(n-1)^2 + \frac{1}{12}(n-1)^3\right] \tag{5.30}$$

If the inequality in (5.30) is satisfied, then r_{max} is less than r_f and, using (5.8) and (5.11), the functions f_i and g_i will have the following bounds

$$\frac{-r_i}{2e}(a\cos(\theta_i) - b\sin(\theta_i)) \le f_i \le \frac{r_i}{2e}(a\cos(\theta_i) - b\sin(\theta_i)) \tag{5.31.a}$$

$$\frac{-r_i}{2e}(c\cos(\theta_i) + d\sin(\theta_i)) \le g_i \le \frac{r_i}{2e}(c\cos(\theta_i) + d\sin(\theta_i)) \tag{5.31.b}$$

which simplify to

$$\frac{-r_i}{2e}\sqrt{a^2 + b^2} \le f_i \le \frac{r_i}{2e}\sqrt{a^2 + b^2} \tag{5.32.a}$$

$$\frac{-r_i}{2e}\sqrt{c^2+d^2} \le g_i \le \frac{r_i}{2e}\sqrt{c^2+d^2} \tag{5.32.b}$$

In the terms involving f_i and g_i are multiplicative. Hence, $[r_i \cos(\theta_i) f_i + r_i \sin(\theta_i) g_i]$ is the function that must be examined. If $r_{max} \le r_f$ we can use (5.32) to write

$$r_i \cos(\theta_i) f_i + r_i \sin(\theta_i) g_i \le \frac{r_i^2}{2e}\sqrt{a^2+b^2+c^2+d^2} \tag{5.33}$$

For convenience let

$$M = \frac{1}{2e}\sqrt{a^2+b^2+c^2+d^2} \tag{5.34}$$

Using (5.34) and (5.16) an upper bound of can be written as

$$r_i \dot{r}_i \le -(1+2\alpha_W) r_i^2 + M r_i^2 + \alpha_W r_i (r_{i-1} + r_{i+1}) \tag{5.35}$$

which simplifies to

$$\dot{r}_i \le -(1+2\alpha_W) r_i + M r_i + \alpha_W (r_{i-1} + r_{i+1}) \tag{5.36}$$

Letting $\beta = M - 1$ and

$$\boldsymbol{W} = \begin{bmatrix} \beta - 2\alpha_W & \alpha_W & & & & \\ \alpha_W & \beta - 2\alpha_W & \alpha_W & & & \\ & \alpha_W & \beta - 2\alpha_W & \alpha_W & & \\ & & & \cdots & & \\ & & & \alpha_W & \beta - 2\alpha_W & \alpha_W \\ & & & & \alpha_W & \beta - 2\alpha_W \end{bmatrix} \tag{5.37}$$

we rewrite (5.36) as

$$\dot{\boldsymbol{r}} \le \boldsymbol{W}\boldsymbol{r} \tag{5.38}$$

Using the same logic which leads to (5.19), let

$$\dot{\boldsymbol{p}} = \boldsymbol{W}\boldsymbol{p} \tag{5.39}$$

and assume that the initial conditions for both systems are identical, i.e. $\boldsymbol{p}(0) = \boldsymbol{r}(0)$, then $\boldsymbol{r}(t) \leq \boldsymbol{p}(t)$ for $t > 0$. If all the eigenvalues of $\boldsymbol{W}$ are negative, then the matrix is stable. If the matrix is stable all the elements of $\boldsymbol{p}$ approach zero, which forces all the elements of $\boldsymbol{r}$ to approach zero. We now examine the eigenvalues of $\boldsymbol{W}$ to find under what conditions they become negative. The eigenvalues of $\boldsymbol{W}$ are given by

$$\lambda_k = (\beta - 2\alpha_W) - 2\alpha_W \cos\left(k\frac{\pi}{n}\right) \tag{5.40}$$

where $k = 1, 2, \ldots n-1$ and $n \geq 3$. The condition for all eigenvalues to be negative can be written as

$$\alpha_W > \frac{\beta}{4\sin^2(\pi/2n)} \tag{5.41}$$

For $n \gg 1$ this becomes

$$\alpha_W > \frac{\beta n^2}{\pi^2} \tag{5.42}$$

In summary, synchrony will be asymptotically stable for the chain of coupled oscillators defined in (5.7) if α_W is chosen such that the inequalities in (5.30) and (5.41) are satisfied. This concludes the proof.

The reported time for a human subject to identify a single object is estimated to be less than 100 ms. [Biederman, 1987]. If oscillatory correlation is used by the brain, synchrony must be achieved before identification takes place. Experimental evidence from the cat visual cortex shows that synchrony is achieved quickly, within 25-50 ms., or 1-2 cycles in 40 Hz oscillations [Gray et al., 1991]. These experimental results emphasize the importance of fast synchrony. From practical considerations synchrony must also be achieved quickly in order to deal with a rapidly changing environment. In this model we can control the rate of synchrony by increasing the coupling strength. But that would lead to unreasonably large values for α_W. This problem can be avoided by careful adjustment of the nullclines, and we now describe a method by which a chain of several hundred W-C oscillators, as defined in (5.1), but arranged as a one dimensional chain, can be entrained within the first cycle.

Our method of fast synchrony requires that there exist one region in the phase plane where the x and y nullclines of the oscillator are very near to one another. More specifically, in the system of (5.1), the parameters were chosen so that this occurs in the upper left hand corner, as seen in Figure 55. The oscillators travel slowly through this region because, close to the nullclines, the values of $\dot{x}$ and $\dot{y}$ are near zero. Note that this need not be true in general, but it is true in the smoothly varying W-C equations that we use. The x and y nullclines are so near each other that only a small perturbation is needed to push the y nullcline to the left, and cause it to intersect the x nullcline (we will use the coupling term to create this perturbation). When the nullclines intersect, two new fixed points are

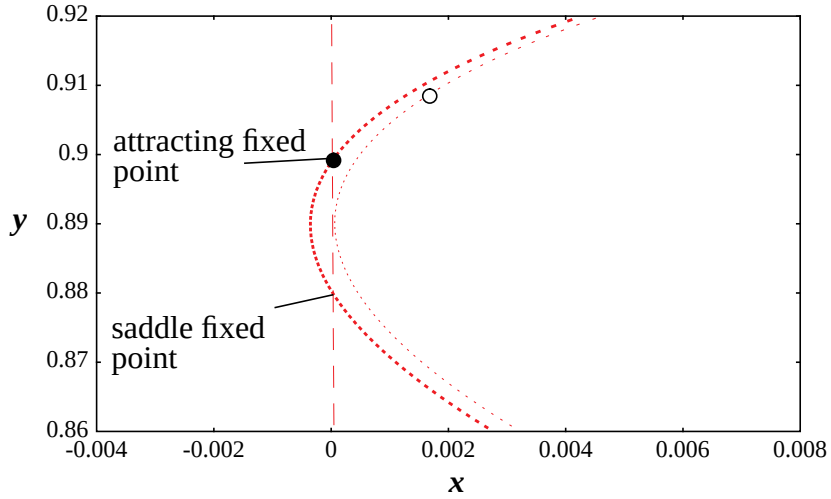

Figure 58. An enlarged diagram of the upper left hand corner of Figure 55 that displays the nullclines of two interacting oscillators. The two dashed curves are the nullclines for the leading oscillator, and the black filled circle represents the position of the leading oscillator. The interaction term causes the y nullcline (short dashed curve) of the leading oscillator to be perturbed to the left so that it intersects the x nullcline (long dashed curve). This creates an attracting fixed point, and a saddle fixed point. The interaction term does not impede the motion of the trailing oscillator (open circle), which will approximately follow the path given by the solid curve. The leading oscillator will be trapped at the attracting fixed point until the distance between the oscillators is very small.

created. One of these fixed points is attracting, and will stop periodic motion. We neglect the case when the nullclines just touch, as the single bifurcation point exists only momentarily, and does not significantly affect the dynamics.

Let us examine the case of two coupled oscillators in detail. Specifically, we examine two oscillators that are near to one another and approaching the upper left hand corner of the unit square from the right, i.e. rotating counterclockwise. Figure 58 displays an enlarged picture of this region. The interaction term will cause the x and y nullclines of the leading oscillator to intersect, effectively trapping it at the newly created fixed point. In Figure 58 the leading oscillator (black filled circle) is shown trapped at the attracting fixed point, which is the top intersection of the x nullcline and the y nullcline. The other oscillator is represented by an unfilled circle, and its movement along the limit cycle is not impeded. As the oscillators come closer the interaction term decreases, and the y nullcline of the leading oscillator moves to the right. When the oscillators are close enough, the x and y nullclines of the leading oscillator will separate, releasing the leading oscillator from the fixed point and allowing its motion along the limit cycle to continue. We have ignored the motion of the x nullcline because it moves up and down only a small amount during this process. Since the x nullcline is almost completely vertical in this region, moving it by a small amount has a negligible effect. In summary, our method of fast synchrony

requires that there be a region such that the parameters are near a saddle bifurcation, and that the interaction terms be organized to alter the behavior of an oscillator in this region appropriately as described above.

The distance between the oscillators can be controlled precisely in this manner. It depends solely on the original separation of nullclines, and the size of α_W. To be more precise, for the parameters specified in the caption of Figure 55, a y interaction term greater than 0.0003 will cause the nullclines to intersect. Thus, the distance between the oscillators in the y direction, $(y_2 - y_1)$, will have to be less than $(0.0003/\alpha_W)$ before periodic motion resumes. Because the oscillators are almost directly above one another, $x_2 \approx x_1$, and the distance between the oscillators can be approximated by $(0.0003/\alpha_W)$. This distance is orders of magnitude smaller than the size of the limit cycle, so we can safely call the oscillators separated by this distance synchronized. However, this phase adjustment only occurs in the upper left hand corner of the limit cycle. One must ensure that both oscillators are in this region and not on opposite sides of the limit cycle. We increase the value of α_W to make sure the oscillators approach each other before moving to the limit cycle. This behavior can be explained by examining only the interaction terms in (5.1), and ignoring the oscillatory terms. We find that the scalar diffusive coupling terms converge asymptotically to a single stable point. Thus, if α_W is sufficiently large, the interaction terms will dominate over the oscillatory terms, and cause the oscillators approach each other. As the oscillators come together, the interaction terms decrease, and the oscillatory terms start to contribute to the dynamics. So, with a sufficiently large α_W, the oscillators will be loosely synchronized before oscillatory motion starts. The oscillators will then approach the upper left hand corner of the limit cycle. If the distance between the two oscillators is larger than $(0.0003/\alpha_W)$, then the interaction term will cause the nullclines of the leading oscillator to intersect. An attracting point will be created and the leading oscillator will be trapped at this point until the second oscillator moves to within a distance of $(0.0003/\alpha_W)$. In summary, α_W is used to loosely group the oscillators together. The oscillators then travel along the limit cycle to the upper left hand corner, where they become tightly synchronized.

By controlling α_W, and the position of the nullclines, we can reduce the distance between the two oscillators to an arbitrarily small value. Using these same techniques, we can control the overall entrainment of a chain of oscillators. Figure 59 shows the x activities of 34 oscillators plotted on the same graph. The oscillators are those defined in (5.1), but they are arranged in a chain, and are not connected to GI. The strong interaction terms cause the oscillators to approach each other rapidly, creating a thick conglomeration of curves, instead of 34 completely random curves. These loosely synchronized oscillators will then approach the upper left hand corner of the limit cycle, where they become tightly synchronized. By the next peak, one can see that only a single thin curve is exhibited, as all the oscillators are at virtually the same x value at the same time. We make no claims that an infinite number of oscillators can be entrained using this method. Large line lengths $(n > 500)$ could require excessively large coupling strengths. We are interested in finite systems, and have tested this method with chain lengths up to several hundred oscillators. We conjecture that the behavior for a matrix of 256×256 locally coupled oscillators would be similar in terms of their synchronization.

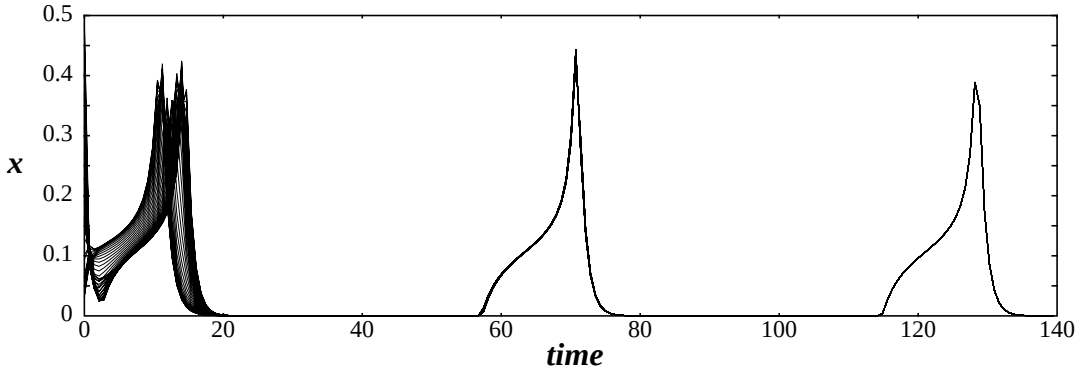

Figure 59. This graph displays the combined x values of 34 oscillators with respect to time. An accurate synchrony is achieved within the first cycle. The random initial conditions used were restricted to the range of the limit cycle, i.e. $0.0 \le x \le 0.5$ and $0.0 \le y \le 1.0$. Parameters $\alpha_W = 90$ and $\sigma = 0$.

The method described above can group many oscillators to within a small distance of one another, and therefore within a small distance of the in-phase solution. Because we have not shown that the actual W-C oscillators synchronize, a variational analysis [Minorsky, 1962] is appropriate. In this analysis all the variables are perturbed by a small amount from a known solution, in this case, the synchronous solution. The perturbations are assumed to be sufficiently small so that their first order approximations are valid. The properties of the resulting system of linear equations can then be examined. We assume the existence of a smooth stable limit cycle, and do not consider the effects of noise or GI. Our analysis has shown that the in-phase solution is locally stable. We omit the details of this straightforward procedure of the analysis.

In summary, we have shown that the piece-wise linear form of the W-C oscillator will synchronize if the coupling strength meets a certain criteria, and we have presented a method for rapid synchrony. In our simulations, we have used both the piece-wise linear approximation of the oscillator (5.7) and the actual W-C oscillators (5.1), and observed that any positive coupling strength will give rise to synchrony, even if it does not satisfy the conditions previously specified. Therefore we conclude that synchrony can be achieved in populations of neural oscillators with local connections.

5.4 Desynchronization

As discussed previously, a method of desynchronization is necessary for minimizing the possibility of accidental synchrony. Several models [Schillen and König, 1991, von der Malsburg and Buhmann, 1992] have methods of desynchronization, but it is not clear how these models perform with more than two objects. In Hansel and Sompolinsky [Hansel and Sompolinsky, 1992], noise in a chaotic system is used to desynchronize objects, but this can also synchronize objects. Hence this is not a reliable method of distinguishing multiple objects.

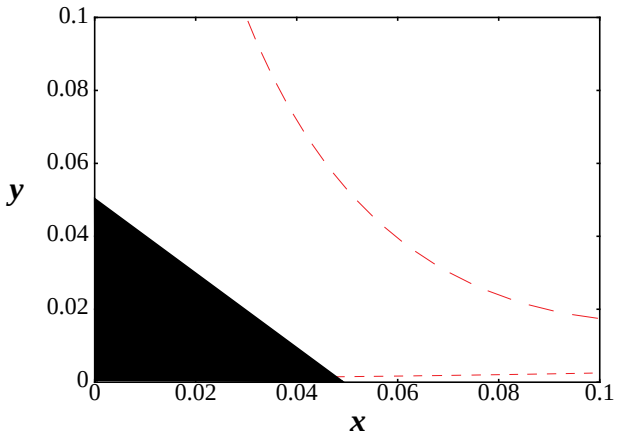

Figure 60. A close look of the triggering region (black filled triangle), the x nullcline (short dashed curve), and the y nullcline (long dashed curve). The value $\mu = 0.048$ was used in the simulations, but other nearby values result in desynchronization also. The other parameters were $U = 2.9$ and $\upsilon = 2.0$.

In order to reliably desynchronize multiple objects, independent oscillations in an oscillator network cannot be permitted. Thus we globally connect GI to and from every oscillator in the network so that no two oscillators act fully independently. These connections serve to adjust phase relationships between oscillator groups representing different objects. GI has a minimum value of zero, and is defined as

$$\dot{z} = U(1-z)\,Tr - \upsilon z \tag{5.43}$$

Tr is a binary value, which is turned on (set to one) if any oscillator lies within a small region near the origin; it is defined as

$$Tr = \begin{cases} 1 & if \;\; (x_i + y_i) < \mu \qquad 1 < i < N \\ 0 & if \;\; otherwise \end{cases} \tag{5.44}$$

The positive parameters U and υ control the rate of growth and decay of z. We call this area near the origin the *triggering region* because when an oscillator enters this region, $Tr = 1$, and the value of GI starts to increase. μ controls the size of the triggering region. As seen in (5.1), the value of GI is fed into the x unit of every oscillator. This manipulation has the simple effect of raising or lowering the x nullcline of every oscillator. Figure 60 displays the triggering region and its position relative to the nullclines. Just to the right of the triggering region there is another slow region, because the x and y nullclines are relatively close. All oscillators rotate counterclockwise, so an oscillator will enter the triggering region, and then pass through the slow region between the nullclines.

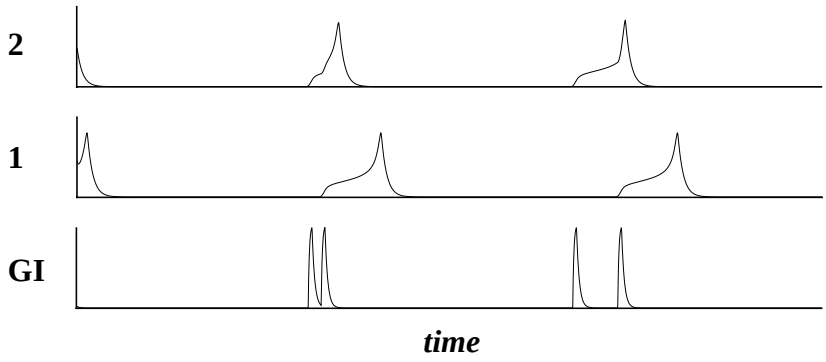

Figure 61. The activities of two oscillators and the global separator are plotted with respect to time. The two oscillators are desynchronized during the second cycle. The shape of the first oscillator is significantly altered because its speed is increased by GI. All parameters are the same as those previously listed in Figure 55 and Figure 60.

GI can only take on positive values, enabling it to raise nullclines or return them to their original positions. An oscillator in the triggering region will cause the x nullcline of every oscillator to rise, and will produce a marked increase the speed of those oscillators in the slow area. Because the triggering region and the slow region are adjacent, any two oscillators with nearby phases will be separated when the trailing oscillator enters the triggering region. The movement of the x nullclines will affect oscillators elsewhere on the limit cycle, but the change in their speed of motion will be negligible compared to the increase in speed received by an oscillator in the slow area.

Figure 61 displays the ability of GI to separate two oscillators. The first two plots display the x activity of two oscillators in time. The third plot is the activity of GI with respect to time. The oscillators are almost in phase in the first cycle, but a major shift occurs during the second cycle. This occurs when oscillator 2, which trails oscillator 1, enters the triggering region and thus excites GI, which then increases the speed of oscillator 1. The sharp change in the characteristic shape of oscillator 1 during the second cycle demonstrates the increase in speed induced by GI while oscillator 1 was within the slow region. Afterward, GI continues to cause minor phase shifts during every cycle. These small phase shifts slowly decrease as the relative phase difference increases. Eventually, an equilibrium is attained. The equilibrium, however, does not ensure an antiphase relationship between the two oscillators, but suffices to clearly distinguish their phases.

Naturally, the desynchronization of objects by this method acts in direct opposition to the necessity of achieving synchrony within groups of oscillators. We resolve this problem by increasing the coupling strength. Increased coupling maintains synchrony within groups of connected oscillators, but does not alter the performance of GI because it does not change the shape of the limit cycle.

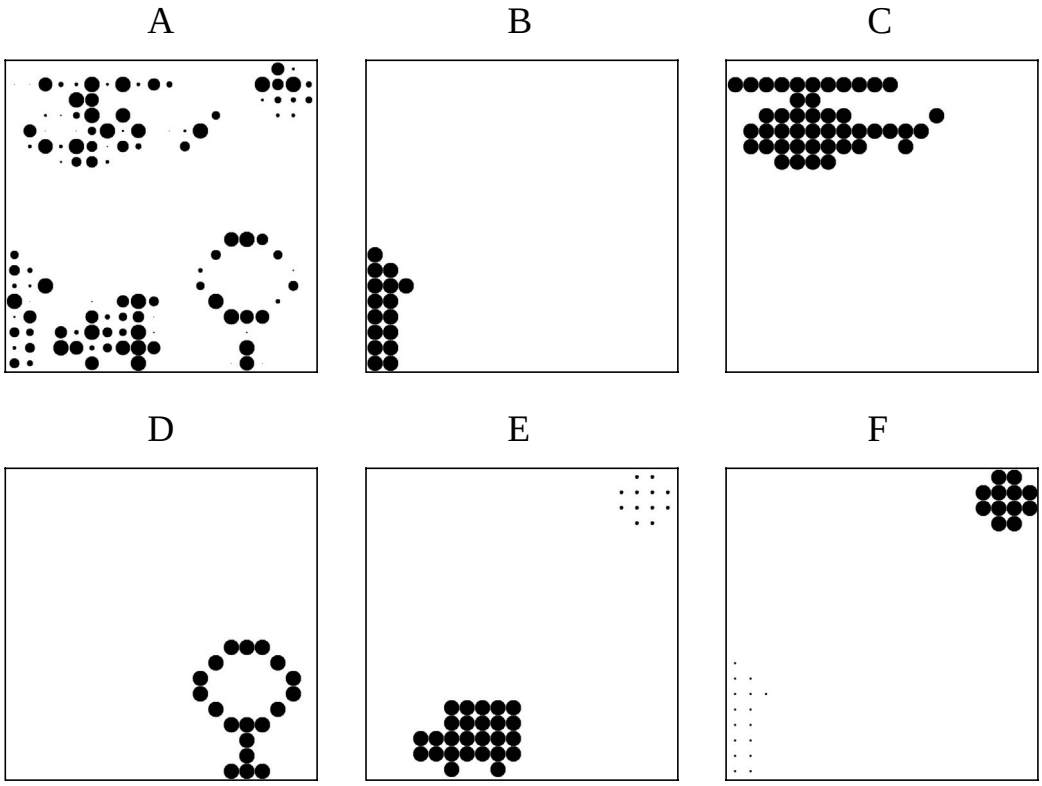

Figure 62. Each picture represents network activity at a time step in the numerical simulation. The size of the circle is proportional to the x activity of the corresponding oscillator. (A) The oscillators have random positions on the phase plane at the first time step. (B)-(F) Successive time steps that correspond to the maximal activities for each group of oscillators. $\alpha_W = 10.0$ in this simulation. The other parameters are as specified in the captions of Figure 55 and Figure 60. The random initial conditions used were restricted to the range of the limit cycle, namely, $0.0 \le x \le 0.5$ and $0.0 \le y \le 1.0$.

5.5 Simulation Results

We now discuss the simulation results of this model using the input displayed in Figure 56. Figure 62A-F display network activity at specific time steps during numerical integration. Figure 62A represents the initial activity of the network. The sizes of the circles are directly proportional to the x values of the corresponding oscillators. The random sizes of the circles in Figure 62A represent the random initial conditions of the oscillators. Figure 62B is a later time step when the object that resembles a house is at its highest activation. Figure 62C displays the time step after Figure 62B when the object resembling a helicopter is maximally active. Figure 62D corresponds to the time step after Figure 62C when the highest activation for the tree-like object is attained. This object was specifically selected to emphasize that any connected region will synchronize, whether it is concave or

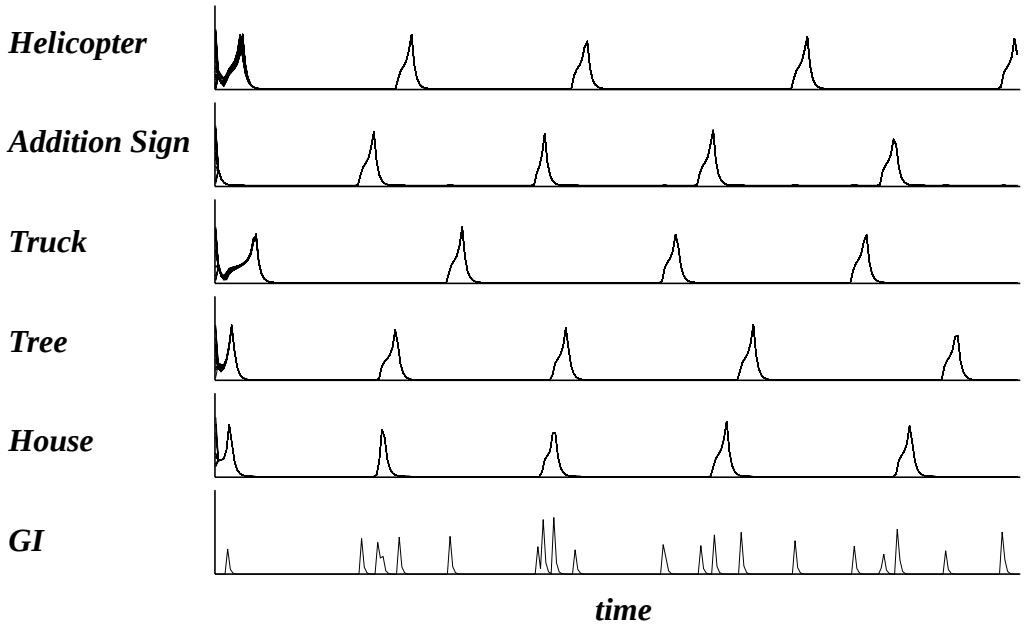

Figure 63. The plot labeled “GI” displays the activity of the global separator with respect to time. The other five plots display the combined x activities of all the oscillators stimulated by the corresponding object. Each of the five oscillator groups is synchronized within the first cycle, and by the second cycle is desynchronized from the other oscillator

convex. Figure 62E shows a later time step when the truck shaped object is maximally activated. The object resembling a thick addition symbol is also weakly activated at this time step. Finally, Figure 62F shows the time step when the thick addition sign is at its highest activation. The objects clearly “pop out” once every cycle.

In Figure 63, we display the activities of GI and the x activities of all stimulated oscillators for the first few cycles. The first five plots display the combined x activities of all oscillators that are stimulated by the five objects. Each of the properties we have described in previous sections are shown in this graph. Initially the interaction terms dominate and cause the oscillators to loosely synchronize. Loose synchrony is seen on the graph by observing that each of plots quickly merge into a thick line. By the second peak, the oscillators have been synchronized to such a degree that only a thin single curve is exhibited. Desynchronization most noticeably occurs during the fourth activation of GI. The phase difference between the oscillator groups representing the house and the addition sign is significantly altered at this time. This shift in phase is signaled by the change in the characteristic shape of the oscillator group representing the addition sign. The activity of GI is displayed on the last frame of Figure 63, . GI is activated when any oscillator, or oscillator group passes through the triggering region. When the oscillators are well separated, GI will be active five times per cycle, signaling successive “pop outs” of the five objects.

Only the first three cycles are depicted in this graph, but as we have tested, synchrony within the oscillator groups, as well as desynchrony between the groups is maintained afterwards without degradation.

We can reliably separate up to at least 9 objects (results not shown). Separating the phases of more objects becomes increasingly difficult for this system. The finite time required for an oscillator to travel through the triggering region, and the finite area affected by GI, constrain the number of objects that can be separated. This limitation seems consistent with the well-known psychological result that humans have a fundamental bound on the number of objects that can be held in their attentional span [Miller, 1956].

Even though noise was not used in the simulations presented here, we have tested the network with various amounts of noise. As expected, the system is robust for small amounts of noise, but cannot tolerate very large quantities. This is because noise by itself can cause the nullclines to intersect and thus interfere with the mechanism we use to synchronize oscillators. The amount of noise the system can tolerate increases with the size of the coupling strength.

We used the numerical ODE solvers found in [Press et al., 1992] to conduct the above simulations. An adaptive Runga-Kutta method was used for most of the simulations reported. The Bulrisch-Stoer method was later used to confirm the numerical results. The network had the same dynamics with either of the integration methods. So it is very unlikely that numerical errors played any significant role in our simulation results.

5.6 Discussion

Our analysis of the W-C oscillator network demonstrates that it contains the basic features necessary to achieve oscillatory correlation. This includes: dynamic couplings, local excitatory connections to synchronize oscillators, and global excitatory connections to desynchronize groups of oscillators. With this simple architecture, we have used the theory of oscillatory correlation, together with the Gestalt principle of connectedness to illustrate sensory segmentation. The model retains information of spatial relationships through local coupling, and does not suffer from the problems of accidental synchrony through the use of a global separator to segregate objects.

Although we have not attempted to simulate the experimental findings of Gray et al. [Gray et al., 1989], the network is neurally plausible. The W-C equations represent the activities of neural groups, and local excitatory connections are consistent with lateral connections widely seen in the brain [Kandel et al., 1991]. The global separator may be viewed as part of an attentional mechanism. Experiments conducted by Treisman and Gelade [Treisman and Gelade, 1980] suggest that if an object has several features, a correct conjunction of those features relies on attention. Thus, if feature binding is achieved through oscillatory correlation, the attentive mechanism may serve to synchronize features into a coherent object, as well as segment different objects. In performing desynchronization, GI may accomplish a task that is fundamental to attention. GI also has structural similarities to a proposed neural attentional mechanism. Crick [Crick, 1984] suggested that the reticular complex of the thalamus may control attention, in part because it has connections both to and from many regions of the cortex. Thus, the reticular complex of the thal-

amus may have influence over widely separated sensory processing regions. With its wide range couplings, GI may have structural, as well as functional, relations to the proposed attentional mechanisms.

We have shown that synchrony can occur in locally coupled oscillators if the coupling is sufficiently large. This is proven using the piece-wise linear approximation to the W-C oscillators. Numerically we observe that synchrony occurs, with local coupling, in the actual W-C oscillators (5.1), as well as our approximation to them (5.7), with any positive coupling strength. This implies that synchrony in such oscillator networks is possible with local connections only. We have also demonstrated a method that can synchronize large numbers of oscillators within the first cycle. The method is based on choosing parameters such that the system is near a bifurcation. This technique is not specific to W-C oscillators, or even scalar diffusive coupling. It should be applicable to other types of oscillators as well. We do not know yet have an estimate for how the rate of synchrony changes with the size of the system.

We also present a mechanism for desynchronization, which can segment up to 9 spatially separate objects. Our mechanism requires only a basic control of speed through a single region of the limit cycle, so it can be transferred to other oscillator models (see also [Wang and Terman, 1995] and [Terman and Wang, 1995]).

The matrix analysis we have done for a chain of oscillators can be extended to analyze higher dimensional oscillator lattices. We conjecture that synchrony can also be achieved in more than two dimensions, with only a positive coupling strength. This is based on simulations that we have done with two dimensional grids that exhibit the same phase locking behavior as we have seen in one dimensional chains. Also, this analysis can be done with lateral connections farther than nearest neighbor connections. In fact, numerical simulations (data not shown) in one and two dimensions show that longer range connections facilitate synchronization. We speculate that analysis with longer range connections would indicate a decrease in the connection strength required to achieve synchrony.

In our model, spatial relationships are preserved through local excitatory coupling. The information contained in these relationships allows us to define objects using the Gestalt principles of proximity and connectedness. Thus any spatially separate object can be segmented, independent of its similarity to other objects in other features. That spatial segmentation is fundamental to perceptual processes is supported by the work of Keele et al. [Keele et al., 1988], who show that spatial location is a basic cue for feature binding.

Aside from explaining what may occur in the brain, oscillatory correlation offers a unique approach to the engineering of pattern segmentation, figure/ground segregation, and feature binding. Due to the nature of the oscillations, only a single object is active at any given time, and multiple objects are sequentially activated. The model can be used as a framework upon which more sophisticated methods of segmentation can be built. For example, the network can be extended to handle gray level input also. Dynamic couplings between excited neighboring oscillators could then be based on the contrast in the gray level of the stimulus. Regions with smoothly changing input would be grouped together, and segmented from regions with boundaries of sharp changes in gray level (see Chapter 2 for an implementation of this).

A unique advantage of using oscillatory correlation for perceptual organization is that the architecture is inherently parallel. Each oscillator operates simultaneously with all the others, and computations are based only on connections and oscillations, both of which are particularly feasible for VLSI chip implementation (for an actual chip implementation exploring phase locking see [Andreou and Edwards, 1994]). It also provides an elegant representation for real time processing. Given the enormous amount of information processing required by sensory processing, a parallel architecture and the potential for VLSI implementation are both very desirable qualities.

Perceptual tasks involving neural oscillations have also been observed in audition [Galambos et al., 1981, Madler and Pöppel, 1987] (see Wang [Wang, 1996a] for a model) and olfaction [Freeman, 1978]. Oscillations have also been explored in associative recall networks [Buhmann, 1989, Wang et al., 1990, Abbott, 1990]. With its computational properties plus the support of biological evidence, this model may offer a general approach to pattern segmentation and figure/ground segregation.